Published in final edited form as:
Chem Biol Drug Des. 2010 January ; 75(1): 29–34. doi:10.1111/j.1747-0285.2009.00907.x.

The X-Ray Structure of Carboxypeptidase A Inhibited by a Thiirane Mechanism-Based Inhibitor

Daniel Fernández[1], **Sebastian Testero**[2], **Josep Vendrell**[1], **Francesc X. Avilés**[1,*], and **Shahriar Mobashery**[2,*]

[1] Departament de Bioquímica i Biologia Molecular, Facultat de Biociències, and Institut de Biotecnologia i de Biomedicina, Universitat Autònoma de Barcelona, E-08193 Bellaterra, Spain

[2] Departament of Chemistry and Biochemistry, University of Notre Dame, Notre Dame, IN 46556, USA

Abstract

The three-dimensional X-ray crystal structure of carboxypeptidase A, a zinc-dependent hydrolase, covalently modified by a mechanism-based thiirane inactivator, 2-benzyl-3,4-epithiobutanoic acid, has been solved to 1.38 Å resolution. The interaction of the thiirane moiety of the inhibitor with the active site zinc ion promotes its covalent modification of Glu-270 with the attendant opening of the thiirane ring. The crystal structure determination at high resolution allowed for the clear visualization of the covalent ester bond to the glutamate side chain. The newly generated thiol from the inhibitor binds to the catalytic zinc ion in a monodentate manner, inducing a change in the zinc ion geometry and coordination, while its benzyl group fits into the S1′ specificity pocket of the enzyme. The inhibitor molecule is distorted at the position of the carbon atom that is involved in the ester bond linkage on one side and the zinc coordination on the other. This particular type of thiirane-based metalloprotease inhibitor is for the first time analyzed in complex to the target protease at high resolution and may be used as a general model for zinc-dependent proteases.

Keywords

M14 family of proteases; mechanism-based inactivation; metallopeptidase; thiirane; X-ray crystallography

Metalloproteases from the M14 family (carboxypeptidases, CPs) are involved in many physiologic and pathological processes such as tissue organogenesis (1–3), acute pancreatitis (4,5), diabetes (6,7), inflammation (8,9), fibrinolysis (10,11), neurologic diseases (12), and cancer (13–16). Circulating forms of CP may be used as prognostic tools for the early detection of cancer and other diseases (17). The M14 family of proteases comprises an extended and complex array of zinc-dependent proteins with wide genomic distribution (18–20). They share with matrix metalloproteases (MMPs; e.g., gelatinases, collagenases, matrilysins, and stromelysins) a similar catalytic mechanism, whereby the catalytic zinc ion predisposes the substrate to turnover with the involvement of a conserved glutamate residue in the active site (21). Notwithstanding the shared features of their respective mechanisms, MMPs are endopeptidases, whereas CPs are exopeptidases that remove the C-terminal residues from peptide substrates.

*Corresponding authors: Shahriar Mobashery, mobashery@nd.edu; Francesc X. Avilés, francescxavier.aviles@uab.es.

Most known small-molecule inhibitors of CPs are chelators of the active site zinc ion. These chelators are often non-discriminant, as their function hinges on coordination with metals. The limited selectivity among potent zinc chelators can be exemplified by thiol-dependent CP inhibitors, such as **1** (2-mercaptomethyl-3-guanidino-ethylthiopropanoic acid, Plummer's inhibitor (22)), which was still found to inhibit other M14 proteases (23). A similar concern has been encountered in the development of MMP inhibitors with subtype selectivity (24). Mechanism-based inactivators ('suicide substrate' or 'k_{cat} inactivator') exploit features of the catalytic mechanisms of the targetted enzymes (25). An innocuous agent is converted to the inhibitory species only within the active site of the target enzyme. Compound **2**, 2-((4-phenoxyphenylsulfonyl)methyl)thiirane, SB-3CT, is a prototypical example. It was designed as a selective gelatinase (MMP-2 and MMP-9) inhibitor. Its unique features include a biphenyl moiety that would fit the S1′ pocket of gelatinases and a thiirane ring able to revert into a thiol group upon enzymic reaction (26,27). The oxirane counterpart to **2** is three orders of magnitude less potent than the thiirane (28).

Chemotherapeutic compounds that may be used as drugs or imaging agents targeted to M14 proteases are highly sought (18,29), and the complexity among CPs calls for the development of selective compounds. Based on the notion that a covalently bound mechanism-based CP inactivator might be an ideal starting point for such an endeavor, a screening of our collection of thiirane-based MMP ligands (~500 compounds) against representative M14 proteases was performed. Unfortunately, these molecules did not prove efficacious in inhibition of these carboxypeptidases. We hasten to add that thiirane-based inhibitors of MMPs have not been amenable to study of their structures in complex with the MMPs by X-ray analysis, hence structural information is currenly lacking (30). In an effort to elucidate the minimal structural motifs for inhibition of carboxy-peptidases by thiirane-based inhibitors, we turned to two examples from the literature. Compound **3** (2-benzyl-3,4-epithiobutanoic acid), as well as its oxirane version, **4** (2-benzyl)-3,4-epoxybutanoic acid), have been reported as mechanism-based inactivators of carboxypeptidase A (CPA) (31–33). An earlier structural determination of CPA in complex with oxirane **4** (34,35) has been reported, although the atomic coordinates have not been deposited. Kinetic results showed that thiirane **3** and oxirane **4** displayed a similar inhibitory potency as CPA inactivators, contrary to the example of gelatinase inhibition by **2**.

We synthesized compound **3** for its study with CPA. Its binding to the active site would allow for the coordination of the thiirane sulfur with the zinc ion, making the thiirane more electrophilic and predisposing it to nucleophilic attack by the active site glutamate. Herein, we report the X-ray structure of the enzyme inhibited by covalent modification with this compound.

Methods and Materials

CPA crystals were grown from a 2 μL:2 μL mixture of enzyme solution (14 mg/mL in 0.02 M Tris, pH 7.5) and precipitant (20% PEG 3350, 0.2 M NH_4Cl, 0.02 M Tris pH 7.0) by the vapor diffusion method. The largest crystals were harvested and transferred to a 2 μL drop containing the reservoir solution plus 10 mM of **3**. Soaking lasted for one week before data collection time, at which no crystal cracking or damage was evident. Crystals were harvested, briefly bathed in cryoprotectant buffer (i.e., the reservoir solution with added 30% glycerol), flash frozen in nitrogen stream and diffracted. Some crystals gave excellent quality diffraction images and that of the highest resolution was used for structure determination by the molecular replacement procedure using native CPA (Protein Database: 2ctb) as the model. Programs from the CCP4 suite were used in different stages of structure determination (36). Extra electron density was clearly evident in the region near the catalytic zinc ion and was easily interpreted as the inhibitor molecule. Further, clear continuous

electron density unequivocally revealed the covalent linkage between the inhibitor and Glu-270 side chain. The agreement between the model and the experimental observations is excellent, as indicated by the crystallographic and refinement statistics (Table 1). Geometric details of inhibitor–enzyme interactions are listed in Table 2.

Results and Discussion

The three-dimensional structure of the complex between CPA, a model zinc-dependent protease, and a thiirane mechanism-based inactivator was solved to 1.38 Å resolution. The CPA crystal structure presented herein is the highest resolution structure for this enzyme, with a nearly 80% data completeness in the highest resolution shell. The structure has been deposited with the PDB with accession code 3i1u. As shown in Figure 1, the existence of continuous electron density between the bound inhibitor and the side chain of the glutamate indicates that Glu-270, corresponding to the conserved active site glutamate of the zinc-dependent proteases, is covalently modified by the inhibitor. The establishment of the covalent bond is accompanied by the opening of the thiirane ring with the attendant coordination of the newly formed thiol group with the catalytic zinc ion in a monodentate manner. This arrangement gives a tetrahedral coordination sphere for the zinc ion, with three ligands from the protein and the thiol from the inhibitor. Because thiiranes are quite stable at physiologic pH, the involvement of the active site zinc ion is essential for the ring opening. The coordinated thiol (likely as a thiolate) is the remnant of the interaction of the thiirane sulfur, before the ring opening. Although inhibitor **3** was prepared as a racemic mixture, the X-ray structure reveals that it is only the 2*S*,3*S*-**3** configuration that fits into the electron density map, indicating that the enzyme is enantioselective in its interaction with the inhibitor. This configuration corresponds to that of the D-amino acid series, in accordance with what has been observed for oxirane **4** (34,35).

When compared to the structure of the native CPA, some conformational changes occur upon inhibitor binding. The catalytically important Tyr-248 (37) and Arg-145 have experienced motion. Tyr-248 has been observed in two conformational states in the several structures available for CPA. One brings it to a hydrogen bonding distance of the bound peptide substrate (the ‘closed’ position) and the other is away from it (the ‘open’ position) (38,39). In the X-ray structure of the inhibited complex, the Tyr-248 phenol group moves from the surface closer to the active site cleft to make a strong hydrogen bond to the carboxylate group of the inhibitor (the bond distance is 2.59 Å; the ‘closed’ position). This carboxylate group, which corresponds to the terminal carboxylate of the peptide substrate, is held in place by hydrogen bonds to the side chain of Arg-145 and Asn-144 Nδ1. The benzyl ring of the inhibitor is buried in the S1′ pocket, thus interacting with Ile-255. This interaction is believed to impart CPA selectivity toward hydrolytic processing of the C-terminal hydrophobic amino acids. In this pocket, residues Leu-203 and Ile-243 make C_H-π interactions with the benzyl ring of the inhibitor. The presence of this benzyl ring displaces the water molecules present in the native CPA S1′ pocket. A superimposition with the related carboxypeptidae B (CPB) reveals that the benzyl moiety would clash with Asp-255 of CPB, which corresponds to Ile-255 of CPA, hence the origin of the likely selectivity for CPA. The Glu-270 side chain conformation, which is covalently tethered to the inhibitor, is approximately *gauche* (as measured by the Cα-Cβ-Cγ-Cδ dihedral angle of −74.4°). These observations point to the fact that little changes in key microenvironments in the binding pocket of the enzyme would allow for an exquisite recognition and binding of the ligand, despite it being configurationally dissimilar to the natural peptide substrate.

The zinc environment is perturbed in the complex. The coordination number of the zinc ion is four in the complex with the inhibitor and the resulting geometry is tetrahedral, with three protein ligand atoms at the base and the thiol sulfur of the inhibitor at the apex of a regular

tetrahedron. The Zn–N distances are equal (2.10 Å and 2.11 Å for His-69 and His-196, respectively), while the Zn–S distance is 2.33 Å. The two Zn–O distances from the side chain of Glu-72, the third coordinating amino acid, differ by almost 1 Å (2.04 versus 3.00 Å). This observation shows that Glu-72 is a monodentate ligand to the zinc ion. The conformation of the glutamate carboxylate is *syn* as the O–C–O–Zn dihedral angle is −2.56°. In the native CPA, the Zn coordination number is five because of the bidentate coordination by Glu-72 (the Zn–O distances are 2.13 Å and 2.26 Å). A water molecule is at the apex of the distorted tetrahedron, at a distance of 2.07 Å. Again, the conformation of the glutamate carboxylate is *syn* (O–C–O–Zn = −1.69°). On the whole, the metal ion environment is perturbed by the inhibitor in the CPA-bound structure.

The inhibitor adopted a *trans* conformation in binding to CPA (the main C_1–C_2–C_3–S_1 backbone dihedral angle is −162.4°). The C_3–C_4 and C_3–S_1 bond lengths are normal, 1.49 and 1.81 Å, respectively. The distance from C_4 to Glu-270 Oε2, 1.61 Å, is longer than the C–O ester bond distances reported in the other CPA structures (34,35). The C_3–C_4–Oε2 bond angle compares favorably to that seen in CPA inhibited by 2-benzyl-3-iodopropanoic acid, a halogen-based covalent inhibitor of CPA: 114.3° versus 113.5° (40). The bond angles to heavy atoms around C_3 average 108.3°, with a minimum of 100.9° for C_4–C_3–S_1. This angle is below the ideal tetrahedral value of 109.5° indicating a distortion of the tetrahedral geometry around C_3 carbon. This carbon atom resides amidst the ester bond to Glu-270 side chain and the zinc-coordinating sulfur, S_1. Whether this distortion would have an effect over the inhibitor binding to the enzyme, and hence to its inhibitory potency, might only be assessed by analyzing compounds structurally related to the inhibitor analyzed here.

In summary, we observed in atomic detail the binding mode of a mechanism-based thiirane inhibitor for CPA. The bound inhibitor fits in the S1–S1′ subsites of CPA, a model metallopeptidase. The high-resolution complex between a zinc-dependent protease and a thiirane-based inactivator has been obtained for the first time, allowing for a complete analysis of the covalently modified protein. This structure constitutes the foundation for future development of additional reagents targeting metallocarboxypeptidases.

Acknowledgments

The work in the USA was supported by a grant from the National Institutes of Health. Financial support from the Ministerio de Ciencia e Innovación, Spain (grant BIO2007-68046), Generalitat de Catalunya (grant 2005SGR-1037) and CAMP project 108830 (VI EU Framework Programme) is gratefully acknowledged. DF thanks the support by the Comissionat per a Universitats i Recerca del Departament d'Innovació, Universitats i Empresa de la Generalitat de Catalunya. We wish to express our gratitude to the local staff at the X13 beamline EMBL-DESY, Hamburg, Germany.

References

1. Marquez-Curtis L, Jalili A, Deiteren K, Shirvaikar N, Lambeir AM, Janowska-Wieczorek A. Carboxypeptidase M expressed by human bone marrow cells cleaves the C-terminal lysine of stromal cell-derived factor-1alpha: another player in hematopoietic stem/progenitor cell mobilization? Stem Cells 2008;26:1211–1220. [PubMed: 18292211]
2. Wang H, Zhou Q, Kesinger JW, Norris C, Valdez C. Heme regulates exocrine peptidase precursor genes in zebrafish. Exp Biol Med (Maywood) 2007;232:1170–1180. [PubMed: 17895525]
3. Zhou Q, Law AC, Rajagopal J, Anderson WJ, Gray PA, Melton DA. A multipotent progenitor domain guides pancreatic organogenesis. Dev Cell 2007;13:103–114. [PubMed: 17609113]
4. Borgstrom A, Regner S. Active carboxypeptidase B is present in free form in serum from patients with acute pancreatitis. Pancreatology 2005;5:530–536. [PubMed: 16110251]
5. Saez J, Martinez J, Trigo C, Sanchez-Paya J, Company L, Laveda R, Grino P, Garcia C, Perez-Mateo M. Clinical value of rapid urine trypsinogen-2 test strip, urinary trypsinogen activation

peptide, and serum and urinary activation peptide of carboxypeptidase B in acute pancreatitis. World J Gastroenterol 2005;11:7261–7265. [PubMed: 16437625]

6. Jeffrey KD, Alejandro EU, Luciani DS, Kalynyak TB, Hu X, Li H, Lin Y, Townsend RR, Polonsky KS, Johnson JD. Carboxypeptidase E mediates palmitate-induced beta-cell ER stress and apoptosis. Proc Natl Acad Sci USA 2008;105:8452–8457. [PubMed: 18550819]
7. Kitagawa N, Yano Y, Gabazza EC, Bruno NE, Araki R, Matsumoto K, Katsuki A, Hori Y, Nakatani K, Taguchi O, Sumida Y, Suzuki K, Adachi Y. Different metabolic correlations of thrombin-activatable fibrinolysis inhibitor and plasminogen activator inhibitor-1 in non-obese type 2 diabetic patients. Diabetes Res Clin Pract 2006;73:150–157. [PubMed: 16458385]
8. Asai S, Sato T, Tada T, Miyamoto T, Kimbara N, Motoyama N, Okada H, Okada N. Absence of procarboxypeptidase R induces complement-mediated lethal inflammation in lipopolysaccharide-primed mice. J Immunol 2004;173:4669–4674. [PubMed: 15383602]
9. Deiteren K, Hendriks D, Scharpe S, Lambeir AM. Carboxypeptidase M: multiple alliances and unknown partners. Clin Chim Acta 2009;399:24–39. [PubMed: 18957287]
10. Rooth E, Wallen H, Antovic A, von Arbin M, Kaponides G, Wahlgren N, Blomback M, Antovic J. Thrombin activatable fibrinolysis inhibitor and its relationship to fibrinolysis and inflammation during the acute and convalescent phase of ischemic stroke. Blood Coagul Fibrinolysis 2007;18:365–370. [PubMed: 17473579]
11. Willemse JL, Hendriks DF. A role for procarboxypepidase U (TAFI) in thrombosis. Front Biosci 2007;12:1973–1987. [PubMed: 17127436]
12. Zhu X, Wu K, Rife L, Cawley NX, Brown B, Adams T, Teofilo K, Lillo C, Williams DS, Loh YP, Craft CM. Carboxypeptidase E is required for normal synaptic transmission from photoreceptors to the inner retina. J Neurochem 2005;95:1351–1362. [PubMed: 16219026]
13. Fialka F, Gruber RM, Hitt R, Opitz L, Brunner E, Schliephake H, Kramer F-J. CPA6, FMO2, LGI1, SIAT1 and TNC are differentially expressed in early- and late-stage oral squamous cell carcinoma – a pilot study. Oral Oncol 2008;44:941–948. [PubMed: 18234543]
14. O'Malley PG, Sangster SM, Abdelmagid SA, Bearne SL, Too CK. Characterization of a novel, cytokine-inducible carboxypeptidase D isoform in haematopoietic tumour cells. Biochem J 2005;390:665–673. [PubMed: 15918796]
15. Ross PL, Cheng I, Liu X, Cicek MS, Carroll PR, Casey G, Witte JS. Carboxypeptidase 4 gene variants and early-onset intermediate-to-high risk prostate cancer. BMC Cancer 2009;9:69. [PubMed: 19245716]
16. Tsakiris I, Soos G, Nemes Z, Kiss SS, Andras C, Szanto J, Dezso B. The presence of carboxypeptidase-M in tumour cells signifies epidermal growth factor receptor expression in lung adenocarcinomas: the coexistence predicts a poor prognosis regardless of EGFR levels. J Cancer Res Clin Oncol 2008;134:439–451. [PubMed: 17922141]
17. Matsugi S, Hamada T, Shioi N, Tanaka T, Kumada T, Satomura S. Serum carboxypeptidase A activity as a biomarker for early-stage pancreatic carcinoma. Clin Chim Acta 2007;378:147–153. [PubMed: 17222396]
18. Arolas JL, Vendrell J, Aviles FX, Fricker LD. Metallo-carboxypeptidases: emerging drug targets in biomedicine. Curr Pharm Des 2007;13:349–366. [PubMed: 17311554]
19. Rodriguez de la Vega M, Sevilla RG, Hermoso A, Lorenzo J, Tanco S, Diez A, Fricker LD, Bautista JM, Aviles FX. Nna1-like proteins are active metallocarboxypeptidases of a new and diverse M14 subfamily. FASEB J 2007;21:851–865. [PubMed: 17244817]
20. Vendrell, J.; Aviles, FX.; Fricker, LD. Metallocarboxypeptidases. In: Messerschmidt, A.; Bode, W.; Cygler, M., editors. Metallocarboxypeptidases. Chichester: John Wiley & Sons, Ltd; 2004. p. 176-189.
21. Lipscomb WN, Strater N. Recent advances in zinc enzymology. Chem Rev 1996;96:2375–2434. [PubMed: 11848831]
22. Plummer TH Jr, Ryan TJ. A potent mercapto bi-product analogue inhibitor for human carboxypeptidase N. Biochem Bio-phys Res Commun 1981;98:448–454.
23. Mao SS, Colussi D, Bailey CM, Bosserman M, Burlein C, Gardell SJ, Carroll SS. Electrochemiluminescence assay for basic carboxypeptidases: inhibition of basic

carboxypeptidases and activation of thrombin-activatable fibrinolysis inhibitor. Anal Biochem 2003;319:159–170. [PubMed: 12842119]

24. Fisher JF, Mobashery S. Recent advances in MMP inhibitor design. Cancer Metastasis Rev 2006;25:115–136. [PubMed: 16680577]
25. Walpole CS, Wrigglesworth R. Enzyme inhibitors in medicine. Nat Prod Rep 1989;6:311–346. [PubMed: 2674783]
26. Ikejiri M, Bernardo MM, Bonfil RD, Toth M, Chang M, Fridman R, Mobashery S. Potent mechanism-based inhibitors for matrix metalloproteinases. J Biol Chem 2005;280:33992–34002. [PubMed: 16046398]
27. Kleifeld O, Kotra LP, Gervasi DC, Brown S, Bernardo MM, Fridman R, Mobashery S, Sagi I. X-ray absorption studies of human matrix metalloproteinase-2 (MMP-2) bound to a highly selective mechanism-based inhibitor. comparison with the latent and active forms of the enzyme. J Biol Chem 2001;276:17125–17131. [PubMed: 11278946]
28. Brown S, Bernardo MM, Li Z-H, Kotra LP, Tanaka Y, Fridman R, Mobashery S. Potent and selective mechanism-based inhibition of gelatinases. J Am Chem Soc 2000;122:6799–6800.
29. Fernandez D, Aviles FX, Vendrell J. Aromatic organic compounds as scaffolds for metallocarboxypeptidase inhibitor design. Chem Biol Drug Des 2009;73:75–82. [PubMed: 19152637]
30. Lee M, Hesek D, Shi Q, Noll BC, Fisher JF, Chang M, Mobashery S. Conformational analyses of thiirane-based gelatinase inhibitors. Bioorg Med Chem Lett 2008;18:3064–3067. [PubMed: 18083555]
31. Kim DH, Chung SJ. Inactivation of carboxypeptidase A by 2-benzyl-3,4-epithiobutanoic acid. Bioorg Med Chem Lett 1995;5:1667–1672.
32. Kim YM, Kim DH. Convenient preparation of all four possible stereoisomers of 2-benzyl-3,4-epoxybutanoic acid, pseudomechanism-based inactivator for carboxypeptidase A via a-chymotrypsin-catalyzed hydrolysis. Bull Korean Chem Soc 1996;17:967–969.
33. Lee SS, Li ZH, Lee DH, Kim DH. (2R,3S)- and (2S,3R)-2-benzyl-3,4-epoxybutanoic acid as highly efficient and fast acting pseudomechanism-based inactivators for carboxypeptidase A: design, asymmetric synthesis and inhibitory kinetics. J Chem Soc Perkin 1995;1:2877–2882.
34. Ryu S-E, Choi H-J, Kim DH. Stereochemistry in inactivation of carboxypeptidase A. Structural analysis of the inactivated carboxypeptidase A by an enantiomeric pair of 2-benzyl-3,4-epoxybutanoic acids. J Am Chem Soc 1997;119:38–41.
35. Yun M, Park C, Kim S, Nam D, Kim SC, Kim DH. The x-ray crystallographic study of covalently modified carboxypeptidase A by 2-benzyl-3,4-epoxybutanoic acid, a pseudomechanism-based inactivator. J Am Chem Soc 1992;114:2281–2282.
36. Collaborative Computational Project, number 4. The CCP4 suite: programs for protein crystallography. Acta Crystallogr D Biol Crystallogr 1994;50:760–776. [PubMed: 15299374]
37. Cho JH, Kim DH, Lee KJ, Choi KY. The role of Tyr248 probed by mutant bovine carboxypeptidase A: insight into the catalytic mechanism of carboxypeptidase A. Biochemistry 2001;40:10197–10203. [PubMed: 11513597]
38. Firth-Clark S, Kirton SB, Willems HM, Williams A. De novo ligand design to partially flexible active sites: application of the ReFlex algorithm to carboxypeptidase A, acetylcholinesterase, and the estrogen receptor. J Chem Inf Model 2008;48:296–305. [PubMed: 18232679]
39. Pallares I, Fernandez D, Comellas-Bigler M, Fernandez-Recio J, Ventura S, Aviles FX, Bode W, Vendrell J. Direct interaction between a human digestive protease and the muco-adhesive poly(acrylic acid). Acta Crystallogr D Biol Crystallogr 2008;D64:784–791. [PubMed: 18566513]
40. Massova I, Martin P, de Mel S, Tanaka Y, Edwards B, Mobashery S. Crystallographic and Computational Insight on the Mechanism of Zinc-Ion-Dependent Inactivation of Carboxy-peptidase A by 2-Benzyl-3-Iodopropanoate. J Am Chem Soc 1996;118:12479–12480.
41. Davis IW, Murray LW, Richardson JS, Richardson DC. MOLPROBITY: structure validation and all-atom contact analysis for nucleic acids and their complexes. Nucleic Acids Res 2004;32:W615–W619. [PubMed: 15215462]

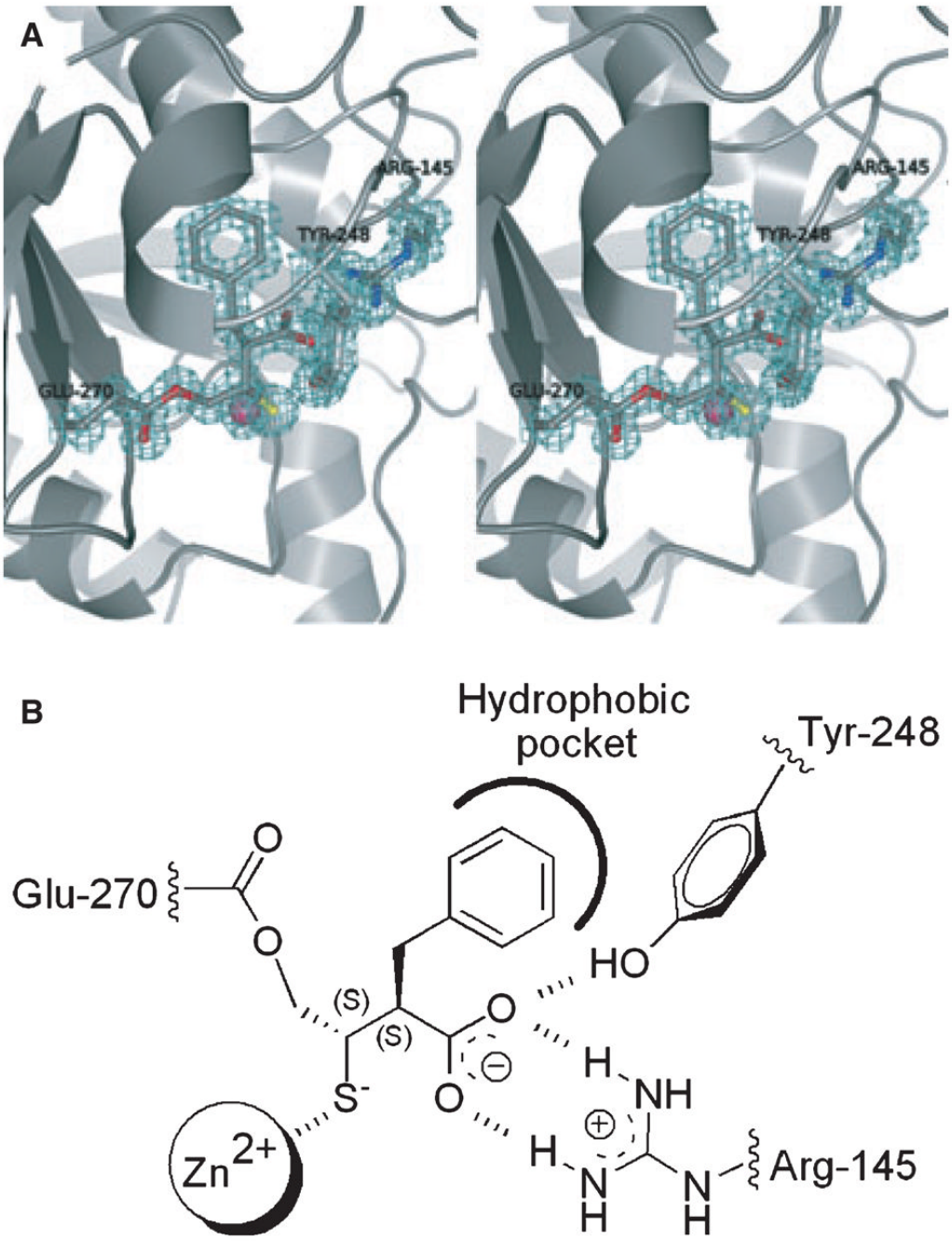

Figure 1.

(A) The structure of the CPA-inhibitor complex. A2$F_{obs}-F_{calc}$ electron density map showing the CPA active site with the product of the reaction of thiirane **3** with the enzyme. The electron density map (chicken wire), calculated deleting the Glu-270 side chain and inhibitor coordinates, is contoured at a 1.5σ level. The inhibitor and residues important for binding are shown in capped sticks and are labeled. The catalytic zinc ion is in magenta, while the sulfur atom from the inhibitor is in yellow. Other atoms are colored blue (nitrogen) and red (oxygen). A continuous electron density is clearly seen along the bond linking Glu-270 side chain and the inhibitor. (B) Schematic representation of the CPA-inhibitor complex.

Table 1

Statistics of data collection and refinement for inhibitor-bound CPA

Parameters	Value
Wavelength used during data collection	0.8123 Å
Unit cell constants	a = 42.32 Å, b = 57.50 Å, c = 57.08 Å
	α = 90.0°, β = 99.1°, γ = 90.0°
Resolution range	31.27–1.38 Å
Space group	$P2_1$ (1 mol/asymmetric unit)
Number of measured reflections	488 546
Number of unique reflections	54 345
R_{merge}[a] (overall/outermost shell)	6.8/37.9%
Completeness & multiplicity (overall/outermost shell)	96.6/77.8% 6.1/5.3
I/σI (overall/outermost shell)	8.8/1.8
Reflections used for refinement (total/test set)	52 590/1102
Crystallographic R_{factor}[b]/R_{free}[c]	14.3/15.7%
Deviation from ideality	
r.m.s.d. bond lengths	0.008 Å
r.m.s.d. bond angles	1.14°
Number of protein atoms/total atoms	2438/2930
B-factor statistics (Å^2)	
Overall *B*-factor/Wilson plot *B*-factor	10.7/9.3
Catalytic domain, main/side chain	7.3/8.4
Zn^{2+} (1 in total/1 mol per monomer)	5.3
Inhibitor atoms (14 in total/1 mol per monomer)	5.8
Glycerol atoms (42 in total/7 mols per monomer)	19.4
Solvent atoms (435 in total)	26.0
Protein geometry[d]	
Ramachandran favored	97.3% (293 of 301 residues)
Ramachandran allowed	99.7% (300 of 301 residues)
Ramachandran outliers	0.3% (1 of 301 residues, Ser-199)
Residues with bad bonds/angles	0.00/0.00%
Rotamer outliers	0.77%

[a] $R_{merge} = \Sigma_{hkl}\,\Sigma_{j=1}$ to $N\,|I_{hkl} - I_{hkl}(j)|/\Sigma_{hkl}\,\Sigma_{j=1}$ to $N\,I_{hkl}(j)$, where N is the redundancy of the data. The outer-most shell is 1.46–1.38 Å.

[b] $R_{factor} = \Sigma_{hkl}\,||F_{obs}| - |F_{calc}||/\Sigma_{hkl}\,|F_{obs}$ where F_{obs} and F_{calc} are the observed and calculated structure factor amplitudes of reflection hkl.

[c] $R_{free} = R_{factor}$ for a randomly selected 2% subset of reflections that were not used in refinement.

[d] According to Molprobity (41).

Table 2

Geometric details inhibitor–CPA interactions

Interaction	Parameter (Å, °)	Comments
Zn/His-69, Zn/His-196, Zn/Glu-72-Zn, Zn/S_1	2.10, 2.11, 2.04, 2.33	Zinc coordination sphere
Glu-270 Oε2-C_4	1.61	Covalent bond to nucleophile Glu-270
Tyr-248 OH-COOH	2.59	Hydrogen bond phenolic ring
Arg-145 Nη1-COOH	2.89	Salt bridge
Arg-145 Nη2-COOH	2.78	
Arg-127 Nη2-COOH	3.35	Hydrogen bond of inhibitor COOH
Asn-144 Nδ1-COOH	2.97	
Leu-203 Cδ1-C_{phenyl}	3.85	Hydrophobic interactions of the benzyl ring (selected)
Ile-243 Cδ1-C_{phenyl}	3.42	
Thr-268 Cγ2-C_{phenyl}	3.68	
C_3–S_1, C_4–C_3–S_1	1.81, 100.9	Geometry around the sulfur